Modulating the extent of fast and slow boron-oxygen related degradation in Czochralski silicon by thermal annealing: Evidence of a single defect

Moonyong Kim,[1] Malcolm Abbott,[1] Nitin Nampalli,[1] Stuart Wenham,[1] Bruno Stefani,[1,2] and Brett Hallam[1]
[1]*School of Photovoltaic and Renewable Energy Engineering, University of New South Wales, Sydney, New South Wales 2052, Australia*
[2]*School of Engineering, Federal University of Rio Grande do Sul, Porto Alegre, Brazil*

(Received 14 December 2016; accepted 25 January 2017; published online 7 February 2017)

The fast and slow boron-oxygen related degradation in p-type Czochralski silicon is often attributed to two separate defects due to the different time constants and the determination of different capture cross section ratios (k). However, a recent study using high lifetime samples demonstrated identical recombination properties for the fast and slow degradation and proposed an alternative hypothesis that these were in fact due to a single defect. The study presented in this article provides further experimental evidence to support the single defect hypothesis. Thermal annealing after light soaking is used to investigate the behaviour of subsequent boron-oxygen related degradation. Modifying the temperature and duration of dark annealing on pre-degraded samples is observed to alter the fraction of fast and slow degradation during subsequent illumination. Dark annealing at 173 °C for 60 s is shown to result in almost all degradation occurring during the fast time-scale, whereas annealing at 155 °C for 7 h causes all degradation to occur during the slow time-scale. This modulation occurs without changing the total extent of degradation or changing the capture cross-section ratio. The results are consistent with the fast decay being caused by defect formation from immediately available defect precursors after dark annealing, whereas the slow degradation is caused by the slow transformation of another species into the defect precursor species before the more rapid reaction of defect formation can proceed. *Published by AIP Publishing.*
[http://dx.doi.org/10.1063/1.4975685]

I. INTRODUCTION

The presence of both oxygen and boron in p-type Czochralski silicon causes a significant reduction of minority carrier lifetime after carrier injection via either current injection or exposure to illumination.[1] The full extent of lifetime degradation typically occurs within 48 h at room temperature and can lead to performance losses approaching 10% in finished devices.[1,2] The reduction of carrier lifetime has a characteristic of proceeding in two stages, with a fast but generally small decay of carrier lifetime, followed by a slower but much more significant decay.[3–7] In studies investigating the extent of degradation on the boron-doping concentration, a linear dependence was observed for both the fast and slow degradation.[4,8]

Thermal annealing in the dark on a degraded sample can lead to a recovery of minority carrier lifetime, although the improvement is not stable.[1,2,9–11] As a result, exposure to subsequent illumination will again cause a degradation of carrier lifetime. The recovery rate for lifetime has been intensively investigated to determine the attempt frequency and activation energy, although there is a significant spread in the values reported.[3,4,12–17] A known condition to fully recover the boron-oxygen (B-O) related degradation is to anneal at 200 °C for 10 min in the dark.[18] This condition has been used in a large number of studies investigating B-O related degradation behaviour.[4,11,13,19–22] Numerous other studies have also used a temperature of 200 °C for dark annealing, although for longer durations ranging from 20 min to 100 h.[6,8,23–29] Other studies have used different temperatures in the range of 210 °C–300 °C (Refs. 30–33) and also 100 °C–400 °C.[34] For the kinetics of the recovery process, one study observed a two-staged recovery of carrier lifetime for the fast decay and a single-staged recovery for the slow decay,[4] while another study reported that the lifetime recovery occurred in one stage for both the fast and slow decay.[3] However, none of the above studies investigated the influence of modulating the dark annealing temperature on the fast and slow degradation behaviour.

The current consensus in the literature is that the fast and slow B-O related degradation effects are caused by two different defects, namely, the fast-forming recombination center (FRC) and the slow-forming recombination center (SRC).[3,4,27,35–37] This hypothesis was proposed due to the differing time constants for the fast and slow degradation and the determination of a different capture cross-section ratio (k) for the fast and slow decay.[4] In particular, assuming a single level for the defect, a k value of approximately 100 was determined for the fast decay, and a much smaller value of approximately 10 was determined for the slow decay.[4] Subsequent studies have refined the k values for the FRC in the range of 65–86.[38] Furthermore, it was proposed that the two defects are independent from one another. That is, the fast reaction does not precede the slow reaction.[4] On this basis, multiple subsequent theories have assumed that two separate defects are responsible for the fast and slow decay in carrier lifetime.[35,38–41]

In our recent work, we observed identical recombination properties of fast and slow degradation with a k value of approximately 19 of the donor level,[42] substantially lower than that observed for fast degradation in earlier studies. A subsequent study by Niewelt *et al.* confirmed this much lower k value for the donor level of fast degradation, obtaining a value of 18.[43] We suggested that the higher k value for the fast decay in earlier studies might have been influenced by the dissociation of iron-boron pairs, given the known behaviour and recombination activity of interstitial iron and iron-boron pairs.[44] With identical recombination properties for the fast and slow degradation, it was proposed that both could be caused by a single defect.[42] Furthermore, preliminary data demonstrated that changing the duration of dark annealing at 200 °C on pre-degraded samples could modulate the normalised defect density of samples within first 1000 s of subsequent illumination.[42] This provided a further link for the fast and slow degradation being caused by the same defect. This was also supported by kinetic modelling, whereby multi-stage degradation of carrier lifetime was presented using a single defect.[42] For this degradation model, it was proposed that a certain population of defect precursors exist in the silicon, and they can immediately form defects when exposed to illumination, resulting in the fast degradation. However, another species also exists in the silicon that can undergo a slow transformation into the defect precursor species before defect formation can proceed.

In this study, we investigate the influence of dark annealing conditions on the behaviour of B-O related degradation during subsequent illumination using *in-situ* lifetime measurements to monitor both the fast and slow decay in carrier lifetime. By changing the temperature and duration of dark annealing, the fraction of fast and slow degradation can be modulated. With appropriate processing, a wafer can have almost all lifetime decay occurring in the fast-degradation regime or in the slow-degradation regime. This modulation occurs without modification to the extent of total degradation. Furthermore, regardless of whether the decay of carrier lifetime occurs largely during the fast or slow timescale, the k value remains unchanged. This implies that regardless of the rate of defect formation (fast or slow), a single recombination active defect type is responsible for the lifetime degradation.

It should be noted that in this work, we adopt the terminology of the annihilation of B-O defects to describe the transition from a "degraded" state into a "dark annealed" state. This refers to either the dissociation of a B-O complex into individual components of boron- and oxygen-related species assuming a diffusion based mechanism for defect formation or the transformation of the recombination active B-O complex into a recombination inactive B-O defect complex assuming a latent defect theory.[45]

II. SAMPLE PREPARATION AND EXPERIMENTAL METHODS

Symmetrical lifetime test structures were fabricated on approximately 200 μm thick boron-doped Cz silicon wafers with a doping density of $N_a = 9.1 \times 10^{15}/cm^3$. Samples were textured in an alkaline solution to remove approximately 10 μm from each side to remove saw-damage, resulting in a thickness of approximately 180 μm. The samples were then phosphorus pre-gettered by a $POCl_3$ diffusion with a sheet resistance of 40 Ω/sq, followed by the removal of the diffusion in an alkaline texturing solution. Subsequently, the wafers were $POCl_3$ diffused to a sheet resistance of approximately 70 Ω/sq. $POCl_3$ deposition was performed at 795 °C for 25 min with a gas flow of 600 sccm oxygen and 425 sccm $POCl_3$ followed by a drive in the process at 885 °C for 7.5 l of N_2. Subsequently, a low temperature anneal process was applied at 650 °C for 12 h in nitrogen ambient to precipitate any interstitial iron not removed during the gettering step.[46] This resulted in undetectable concentrations of interstitial iron using a known method based on the photoconductance decay.[44]

A 75 nm layer of hydrogenated silicon nitride (SiN_x:H) with a refractive index of 2.08 (Ref. 47) was deposited on both sides of the wafers by plasma enhanced chemical vapour deposition (PECVD) in a Roth&Rau MAiA system. As hydrogen is known to lead to a permanent passivation of B-O defects,[48] the samples were not fired. This therefore suppressed any permanent passivation of B-O defects during the illuminated processes.

The samples were initially annealed at 200 °C for 10 min on a hotplate to obtain the lifetime of the samples when B-O defects are completely annihilated. A metal plate with a vacuum was used to ensure good thermal contact to the hotplate and adequate temperature control. Throughout dark annealing, the temperature was monitored using a contact thermocouple, resulting in temperature fluctuations within ±1 °C. Subsequently, the samples were light soaked for 48 h under 0.2 Suns illumination at approximately 35 °C to form all B-O defects and obtain the lifetime of the samples in the fully degraded state.[14]

After full degradation, the samples were annealed at various temperatures for various times (Table I) to investigate the impact of the annealing on the B-O related degradation. Subsequently, light soaking was performed at room temperature with *in-situ* lifetime measurements.

All wafers were characterised using a Sinton Instruments WCT-120 quasi-steady-state photo-conductance (QSS-PC) tool[49] and analysed using the generalised technique.[50] *In-situ* lifetime measurements were recorded throughout the degradation process with a bias light (0.02 Sun intensity),[14] which remained on during the *in-situ* measurements. The lifetime curves were corrected for the bias-light. For all lifetime measurements, an excess carrier concentration of $\Delta n = 0.1 \cdot N_a$ was

TABLE I. Dark annealing time and temperature conditions.

Set	T (°C)	Time (s)
A	127, 135, 155, 173, 192	600
	200	10
B	200	50, 100, 200, 600, 700, 1000
C	200	3600
	226, 266	600
	229, 300	20

used. A Sinton Instruments WCT-120TS in a light-tight box was used to measure the injection level dependent lifetimes of samples at elevated temperature for *in-situ* lifetime measurements investigating the annihilation rate of B-O defects. For this process, samples were left in the dark (no bias-light) between measurements.

From the effective minority carrier lifetime measurements, the normalised defect density, $N^*(t)$, was determined using the following equation:[51]

$$N^*(t) = \sigma_n v_n N_t(t) = \frac{1}{\tau_{LS}(t)} - \frac{1}{\tau_{DA}}, \quad (1)$$

where $N^*(t)$ is the normalised defect density, σ_n is the electron-capture cross-section of the recombination active defect, v_n is the thermal velocity of electrons, $\tau_{LS}(t)$ is the effective lifetime after t seconds of illumination, and τ_{DA} is the effective lifetime in the dark annealed state (after annihilation of the B-O defects). Using the above equation, the saturated normalized defect density, N^*_{LS}, can be defined by

$$N^*_{LS} = \frac{1}{\tau_{DG}} - \frac{1}{\tau_{DA}}, \quad (2)$$

where τ_{DG} is the effective lifetime after full degradation. Using $N^*(t)$ and N^*_{LS}, fractional defect densities (*FDD*), which represent the percentages of B-O defects that were formed respective to the total amount of defects after full degradation, were calculated using the following equation:

$$FDD = \frac{N^*(t)}{N^*_{LS}}. \quad (3)$$

To analyse lifetime curves, the data were corrected for intrinsic recombination. For Auger recombination, the Richter model was used.[52] In order to model the Shockley-Read-Hall (SRH) recombination characteristics of the BO defect, a two-level defect model was used.[53,54] For the donor level of the defect, a trap energy level, $E_{trap,d}$, at 0.41 eV below the conduction band (E_c) was used.[4] The k value associated with the donor level, k_d, was allowed to vary. For the acceptor level of the defect, a trap energy level, $E_{trap,a}$, at 0.26 eV above the valence band, E_v,[53] was used with a fixed k value of $k_a = 2.55 \times 10^{-3}$. The ratio of the electron capture cross section of the donor level to the hole capture cross section of the acceptor level, $k_{de/ah}$, was likewise assumed to be $k_d/215$.[53]

The time-resolved inverse SRH lifetime associated with the BO defect was described by the method of Rein *et al.*[55] For this, the injection level dependent lifetime curve after dark annealing (with full annihilation of BO defects) was subtracted from that after light soaking using Eq. (2) for each injection level.

III. RESULTS AND DISCUSSION

A. Impact of pre-annealing conditions

Thermal annealing was observed to greatly impact the behaviour of B-O related degradation during subsequent illumination. Figure 1 shows the *FDD* of samples during the first

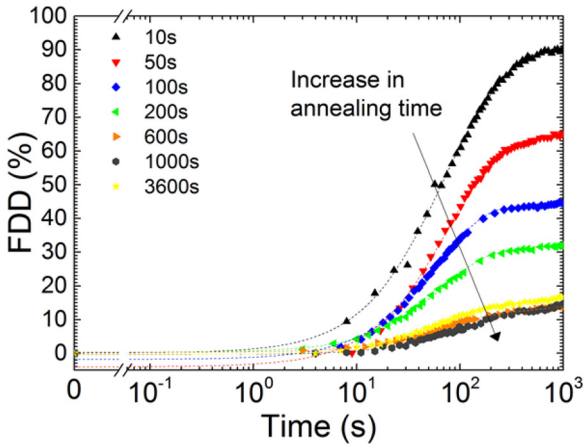

FIG. 1. Fractional defect densities (*FDD*) from *in-situ* lifetime measurements obtained during the first 1000 s of illumination after dark annealing at 200 °C for various durations.

1000 s of illumination after dark annealing at 200 °C for various durations on pre-degraded samples. This value represents an approximate value for the fraction of degradation that occurs on the fast time-scale before the slow degradation has any significant influence. It should be noted that continuing the degradation to 48 h results in a value of approximately 1, consistent with the value of full degradation prior to dark annealing.

As shown, using the standard dark anneal of 10 min duration at 200 °C, a *FDD* after 1000 s of illumination (FDD_{1000s}) of 10% was observed. In contrast, for short dark annealing durations (such as 10 s), approximately 90% of defects were able to form within the first 1000 s, and hence, almost all degradation proceeds in the fast time-scale. Increasing the duration of dark annealing was observed to decrease the FDD_{1000s} values. With 1000 s of dark annealing, only 10% of degradation occurs within the fast time-scale, identical to that achieved for 10 min of dark annealing, indicating that a steady-state had been reached.

A similar trend to the result above was observed for samples annealed for a fixed time period (600 s) at various temperatures. As shown in Figure 2, at a temperature of 155 °C, an FDD_{1000s} of approximately 70% was obtained as compared to a temperature of 229 °C in which the FDD_{1000s} at a similar annealing time was only 10%. Interestingly, annealing at slightly higher temperatures (266 °C and 340 °C) resulted in slightly larger FDD_{1000s} values. This may suggest a thermally activated pathway counteracting the reduction in FDD_{1000s}. At the lowest temperature used, 136 °C, the dark anneal was not able to fully recover the lifetime, with approximately 40% of defects still active before exposure to subsequent illumination.

The response of pre-degraded samples to short and/or low temperature annealing provides insight into the nature of the carrier-induced defect formation. We interpret these results using a single defect hypothesis with two stages of formation. When dark annealing is performed on pre-degraded wafers, first, the defects are annihilated, which recovers the lifetime of the silicon. This leaves the defect precursors immediately available for defect formation. However, with

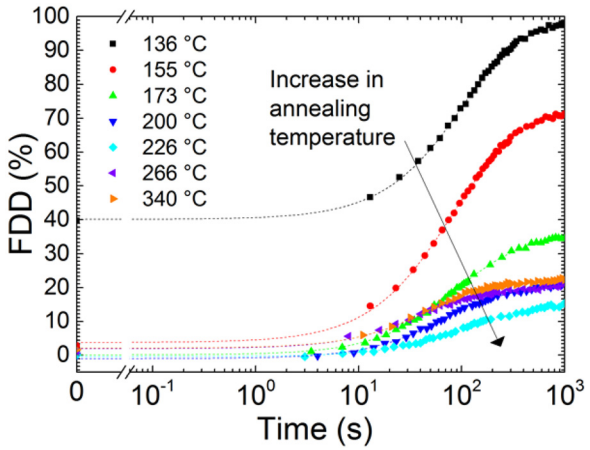

FIG. 2. Fractional defect densities (*FDD*) from *in-situ* lifetime measurements obtained during the first 1000 s of illumination after dark annealing at various temperatures for a duration of 600 s.

prolonged annealing, a further change occurs that transforms the precursors into a more stable state, thus reducing the extent of rapid-degradation (apparent percentage of FRC or degradation in the fast time-scale) and increasing the extent of slow-degradation (apparent percentage of SRC or degradation in the slow time-scale).

The influence of the previous thermal history during dark annealing was also investigated. For this, two extreme conditions were used for an initial dark anneal on the pre-degraded samples (20 s at either 229 °C or 300 °C), both followed by traditional dark annealing (10 min at 200 °C). The *in-situ* effective lifetime during the first 1000 s of illumination after each of these anneals is shown in Figure 3. Initially (solid symbols), there was a significant difference in the degradation due to the different annealing conditions used. However, after the subsequent traditional anneal (open symbols), the extent of degradation of the samples was approximately the same, indicating that the ability to shift between

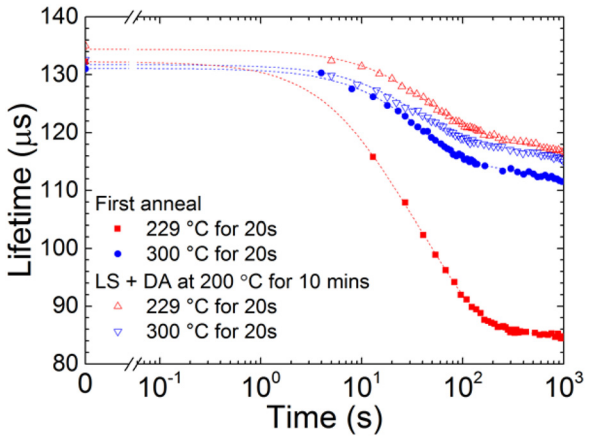

FIG. 3. *In-situ* lifetime measurements during degradation at 300 K under 0.02 Suns illumination for samples with an initial 20 s dark anneal process at either 229 °C or 300 °C (closed symbols) as applied on pre-degraded samples. Corresponding data are shown for the *in-situ* degradation after the previous complete degradation cycle (*LS*), followed by a dark annealing (*DA*) process on both samples at 200 °C for 10 min (open symbols). Note: the legend refers to the condition used for the first anneal.

degradation processes occurring in the fast and slow time-scales is reversible.

The ability to modulate the fraction of fast and slow degradation by thermal annealing suggests that a chemical reaction is taking place in the silicon during dark annealing, beyond simply annihilating the B-O defects and removing their recombination activity. Assuming that there is a reaction taking place, then studying the temperature dependence of the change of the state of the system should allow the determination of an activation energy (E_a) and attempt frequency (ν) for the reaction. The dependence of the *FDD* after 300 s of subsequent illumination (FDD_{300s}) on the duration of dark annealing for temperatures in the range of 127 °C–200 °C is shown in Figure 4. This is equivalent to the fraction of degradation that occurs in the fast time-scale. As shown, for all temperatures, increasing the duration of annealing decreased the FDD_{300s} value. Similarly, shifting to higher temperatures reduced FDD_{300s} for a given duration of dark annealing.

The time constant for the reduction in FDD_{300s} with dark annealing at temperatures in the range of 127 °C–200 °C is shown in Figure 5. Using the Arrhenius equation, this resulted in an attempt frequency of $\nu = 2 \times 10^8$/s and an activation energy of $E_a = 0.91 \pm 0.10$ eV as plotted in Figure 5. This confirms an additional reaction during dark annealing, beyond removing the recombination activity of the B-O defects.

B. Impact of pre-dark annealing on injection dependent lifetime

With the ability to modulate the fraction of degradation due to the fast and slow defects and with the ability to reverse it on a single sample, it is possible to look more closely at the SRH recombination properties. The impact of dark annealing on the capture cross-section ratio, k, was studied on a single sample in which different thermal anneals were applied. Seven annealing conditions were used: the conventional 200 °C process for 10 min, as well as 155 °C for 7 h, 173 °C for 60 s, and 200 °C for 15 s, 100 s, or 600 s. Figure 6 shows the *FDD* determined from *in-situ* lifetime

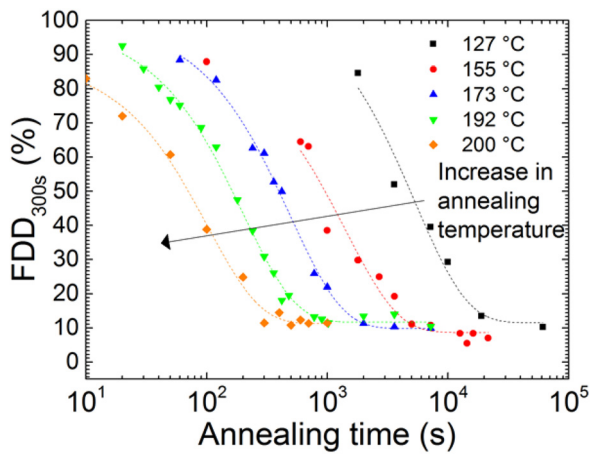

FIG. 4. Fractional defect density after 300 s of light soaking (FDD_{300s}) for various temperatures and durations of dark annealing. Dotted lines are modelling of each temperature with a single exponential decay (from 10% to 90% of FDD_{300s} where the *FDD* saturated to).

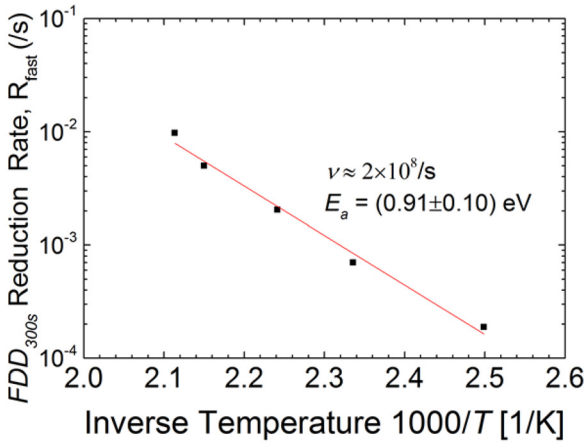

FIG. 5. Arrhenius plot of fast forming defect concentration and pre-annealing temperature. The activation energy $E_a = 0.91 \pm 0.10$ eV and a pre-exponential factor $\nu \approx 2 \times 10^8$/s.

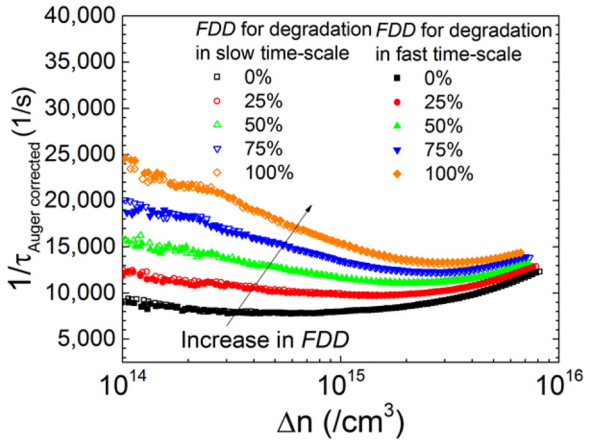

FIG. 7. Auger corrected inverse lifetime vs. injection level curves of a sample measured at various *FDD* values after dark annealing of 155 °C for 7 h (closed symbols) and 173 °C for 60 s (open symbols).

measurements throughout 48 h of subsequent degradation following each annealing process. It is worth noting that identical absolute values of lifetime were observed in the fully dark annealed state ($\tau_{DA} = 125 \pm 1\ \mu$s) and the fully degraded state ($\tau_{DG} = 63 \pm 1\ \mu$s) for every annealing condition used. Hence, modulating the fraction of fast and slow degradation did not change the initial and light-soaked lifetime values.

Injection level dependent effective lifetime curves were analysed at various *FDD* values for all annealing processes used. Figure 7 shows the Auger corrected inverse lifetime curves as a function of excess carrier concentration for two extreme annealing cases: (solid symbols) ~90% of degradation occurring during the fast time-scale (155 °C for 7 h) and (open symbols) ~90% degradation occurring during the slow time-scale (173 °C for 60 s). The initial inverse lifetime curves were identical, indicating, for samples with the same bulk doping density, similar recombination properties in the dark annealed state regardless of whether the majority of degradation will occur in the fast or slow time-scale. Furthermore, at various *FDD* values (0%, 25%, 50%, 75%, and 100%), regardless of the defect formation rates, the inverse lifetime curves were identical.

Further analysis was performed on the fully degraded samples to investigate the k value associated with the degradation with different fractions occurring in the fast and slow time-scales. If the defect that causes degradation in the fast time-scale is the same as that which causes degradation in the slow time-scale, then the recombination activity of samples with different fractions of fast and slow degradation must be identical. Here, annealing at 192 °C was investigated for different durations to result in different *FDD* values after 1000 s of subsequent illumination. The k value of all samples after full degradation, regardless of the fraction of fast and slow degradation, was 19.4 ± 0.5 as shown in Figure 8.

Identical k values were also observed for other *FDD* values between the different annealing regimes. The annihilation rate of the B-O defects at a temperature of 155 °C was compared in Figure 9 on samples with degradation occurring in the fast and slow time-scales. A prior dark anneal at 200 °C of either 15 s or 100 s duration followed by 1000 s of

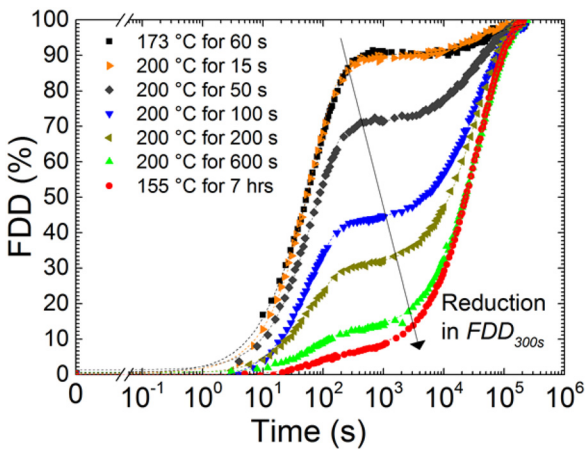

FIG. 6. *FDD* determined from *in-situ* lifetime measurements of after various dark annealing conditions. The dotted lines are fitted with two exponential decay curves.

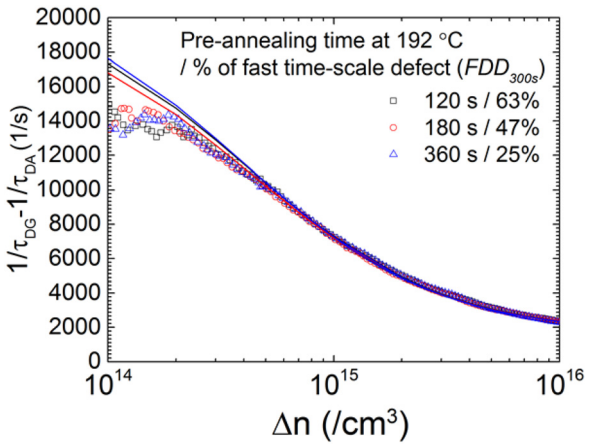

FIG. 8. Curves of Auger corrected inverse effective minority carrier lifetime of ($1/\tau_{DG} - 1/\tau_{DA}$) versus excess minority carrier density (Δn) on samples that were annealed at 192 °C for different durations. τ_{DA} is the initial lifetime after annealing, and τ_{DG} is the final lifetime after 0.2 Suns of illumination for 48 h.

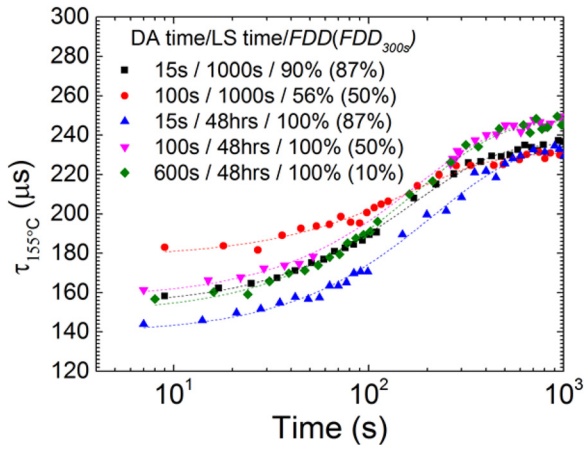

FIG. 9. *In-situ* measurements of lifetime measured at 155 °C. Pre-annealing conditions were varied to vary the fraction of the fast time-scale defect (FDD_{300s}). DA time is the dark annealing time. LS time is the subsequent light soaking time. *FDD* is the initial percentage of total FDD, and FDD_{300s} is the percentage of FDD formed corresponding to fast time-scale of degradation. Dotted lines are the single exponential fit of the lifetime.

illumination resulted in all of the degradation corresponding to the fast time-scale of degradation. Hence, this sample represented the lifetime recovery for degradation occurring in the fast time-scale. A prior dark anneal at 200 °C of 15 s, 100 s, or 600 s duration followed by 48 h of light soaking resulted in complete degradation corresponding ($FDD = 100\%$) to the different fraction of slow time-scale of degradation. Hence, this sample represented the lifetime recovery associated with degradation in the slow time-scale.

Despite whether the samples had fast or slow degradation, the annihilation rate was similar with a single exponential curve, describing the recovery in lifetime. This agrees with the results published by Hashigami *et al.*,[3] although disagrees with the results published by Bothe and Schmidt.[4] This also provides evidence that a single type of defect is being annihilated into a defect precursor.

C. Discussion

The identical recombination properties throughout degradation, regardless of the fraction of fast or slow degradation, strongly suggest that either only a single defect is responsible for both the fast and slow degradation of carrier lifetime or if two different defects are involved, any difference in recombination properties between the defects is negligible. One of the major arguments for the existence of two separate defects in B-O related degradation has been the identification of different recombination properties for the "FRC" and "SRC" in an early study.[4] That early finding now appears to disagree with the recent identification of substantially lower k values for the donor level of what has been attributed to the FRC in multiple studies,[42,43] with now identical recombination properties of that attributed to the SRC.[42] This paper presents further evidence, highlighting identical recombination properties of the fast and slow degradation, what are typically referred to as the FRC and SRC, respectively. In addition, the ability to modulate the fraction of fast and slow degradation by dark annealing, without modulating the total extent of degradation or k value, suggests a strong link between the reactions responsible for both the fast and slow degradation. Further evidence for this link is given, whereby dark annealing first recovers the lifetime of the silicon, allowing the silicon to degrade rapidly during subsequent illumination, with further annealing tending towards a state where the majority of degradation occurs during a slow time-scale. This reaction takes place with an activation energy of $E_a = 0.91 \pm 0.10$ eV and an attempt frequency of $\nu \approx 2 \times 10^8$/s. This suggests that there are at least two recombination inactive states associated with B-O related degradation.

Previously, it was concluded that the FRC is not a precursor of the SRC,[4,20] and therefore, the reaction responsible for fast degradation does not precede the reaction responsible for slow degradation. This understanding is consistent with the findings in this work. It can be presumed that reactions in the B-O defect system are reversible, given the cyclic nature demonstrated between dark annealing and light-soaking[10] and other defect systems such as the iron-boron pair.[44] Taking a fully degraded sample whereby the majority of the degradation occurs in the slow time-scale (SRC) and performing a short dark anneal that is insufficient to fully recover the lifetime do not shift the silicon material into a state where the majority of degradation again occurs in the slow time-scale. Rather, the degradation occurs in the fast time-scale, which is not directly reversible under this model. Therefore, it can be concluded that the reaction causing fast degradation is not a precursor to the reaction causing slow degradation.

Another proposed model discussed a single latent defect species (LC) with two independent paths to form the FRC and SRC but with no direct transition between the FRC and SRC states. However, the FRC was only thought to be responsible for a small *FDD* value, with the extent corresponding to a balance between forward reactions to form the FRC and the reverse reaction towards the LC.[35] Here, we show that dark annealing is able to significantly modulate the fraction of degradation occurring in both the fast and slow time-scale, which would not appear consistent with that model, as there is an ability for an interaction between the degradation that occurs in the fast and slow time-scales and at least two recombination inactive states.

A later model suggested that there are two separate latent defect species in the silicon, one that is a precursor to the FRC and another that is a precursor to the SRC.[38,40,56] This has also appeared in one of the most recent papers discussing defect formation mechanisms.[57] However, this hypothesis is based on having different k values for the FRC and SRC, as well as the latent species being "frozen-in" at relatively high temperatures.[58] This theory would account for the presence of at least two recombination inactive states and however would not account for the ability to shift between the different latent species causing the FRC and SRC as shown in this work.

We recently proposed an alternative model in which the FRC and SRC are in fact the same defect.[42] That is, there is only one recombination active defect responsible for B-O related degradation with identical recombination properties.

The different timescales for degradation are due to the presence of two different recombination inactive states in the silicon. One of these states represents the defect precursor, and the other state is not the actual defect precursor but rather a precursor of the defect precursor. Furthermore, the extent of fast and slow degradation is given by the equilibrium of these two different recombination inactive states. The equilibrium value can be modulated by thermal annealing and hence modulate the extent of fast and slow degradation. This is consistent with the findings in this paper and will be discussed in detail in the Section III D.

D. A kinetic model for defect formation and dark annealing

The understanding presented in this section for a model describing B-O degradation is independent of whether the defect formation mechanism is due to a diffusion-based mechanism to form a B-O complex under illumination or the transformation of a latent B-O complex into a recombination active B-O complex.

We describe the system for defect formation with three states, as shown in Figure 10. States A1 and A2 are recombination inactive, and are equivalent to State A in a conventional three-state model describing the permanent deactivation of B-O defects.[24] State B is the recombination active defect.

We will now use the terminology of state A1 being the Stage 1 defect precursor and state A2 being the Stage 2 defect precursor. The transition from state A1 to state A2 is related to the formation of the Stage 2 defect precursor from the Stage 1 defect precursor. That is, the transition does not directly cause degradation of the silicon as no defects are formed. This transition occurs in the slow time-scale that is normally attributed to the formation of the SRC. This transition is driven both by the availability of electrons and holes and hence carrier-enhanced,[14] with a quadratic dependence on holes.[59] Using reaction rates from the literature, this reaction has an activation energy of 0.475 ± 0.035 eV and an attempt frequency of 4×10^3/s for p-type silicon with a boron doping concentration of 1×10^{16} cm^{-3}.[4] At room temperature, this gives a time constant of 7.5 h. In this work, the time constant for this reaction is estimated at 6.25 h, in close agreement with the previous study.

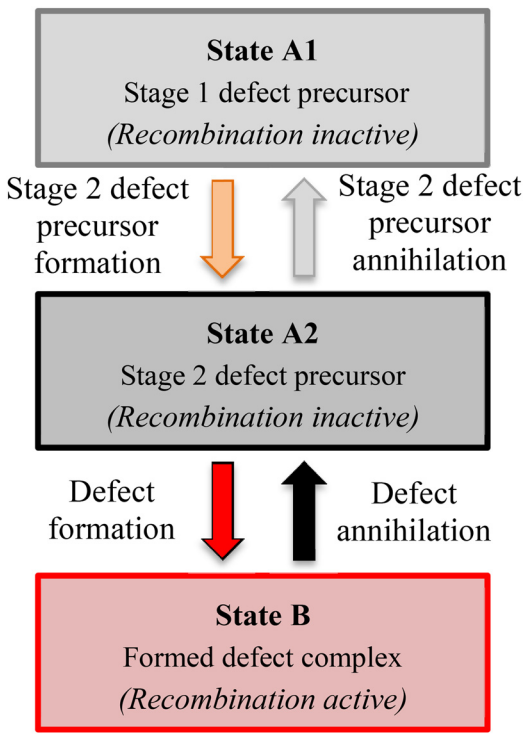

FIG. 10. Diagram of steps of B-O defect formation.

The transition from state A2 to state B is related to defect formation from the Stage 2 defect precursor. This reaction is responsible for the degradation of carrier lifetime. This is a relatively rapid reaction, with a time-scale approximately two orders of magnitude higher than that of the transition from state A1 to state A2 at room temperature. This corresponds to the fast time-scale of degradation. This reaction is also carrier-carrier-enhanced, again with a dependence on the availability of electrons and quadratic dependence on holes.[43] In the literature, this reaction has an activation energy of approximately 0.23 ± 0.02 eV and an attempt frequency of 125/s for p-type silicon with a boron doping concentration of 1.4 Ω·cm,[18] with a corresponding time-constant of 62 s. In this work, the estimated time constant was 65 s.

In this model, the slow reaction (transition from state A1 to state A2) is a precursor reaction of the faster reaction for defect formation (from state A2 to state B). The origin of the multi-stage degradation comes from the silicon material possessing non-zero populations in both states A1 and A2 after dark annealing. Any population starting in state A2, that is a population of available Stage 2 defect precursors, can proceed to defect formation immediately. This is responsible for the fast time-scale of degradation normally attributed to the FRC. On the other hand, any population starting in A1 is not immediately available for defect formation but must first undergo the slow transition into the Stage 2 defect precursor state (A2) before the more rapid defect formation reaction can take place. Therefore, the initial population in state A1 is responsible for the slow degradation that is normally attributed to the SRC. Furthermore, changing the initial fraction of the population in states A1 and A2 changes the extent of degradation that occurs in the fast and slow time-scales. If the entire recombination inactive population is in state A1, then the degradation will proceed with the slow time-scale. If on the other hand, the entire recombination inactive population is in state A2, then the degradation will proceed with the fast time-scale. Typically, after the conventional 200 °C dark annealing process for 10 min, a mix of approximately 90% and 10% will exist in states A1 and A2, respectively, causing most of the degradation to occur in the slow time-scale.

The transition from state B to state A2 represents the annihilation of the B-O defects and therefore the unstable recovery of carrier lifetime that occurs with dark annealing. The literature value for this reaction is $E_a = 1.32 \pm 0.05$ eV and $\nu = 10^{13}$/s.[4] This reaction represents the "dark annealing" reaction in conventional terminology. Only shifting back to

state A2 with a brief dark anneal allows defects to form rapidly during subsequent illumination.

The transition from state A2 to A1 occurs with prolonged dark annealing. This represents the annihilation of the Stage 2 defect precursor into another recombination inactive species, the Stage 1 defect precursor. As determined in this work, the activation energy for this reaction is $0.91 \pm 0.10\,\text{eV}$ with an attempt frequency of $\nu = 2 \times 10^8/\text{s}$. The lower activation energy for this transition than that from state B to A2 suggests that at lower temperatures, it will be easier to recover the lifetime of a degraded sample and move into state A2 than doing so at higher temperatures, which tends to encourage the transition towards state A1. After the transition from state A2 to A1, in subsequent illumination, defects will form in the slow time-scale.

It should be noted that the experimental work in this paper may also suggest the possibility to thermally shift from state A1 to state A2, as indicated by a slight increase in the *FDD* after 1000 s of illumination with increasing dark annealing temperature beyond approximately 230 °C. It is possible that such temperatures are sufficient to thermally generate the free electron concentration required to saturate the electron dependence of the transition from state A1 to A2.

Whilst the data strongly suggests the involvement of a single recombination active defect being responsible for B-O related degradation, it does not directly point to whether the defect formation mechanism is based on a diffusion mechanism or a transformation of a latent (recombination inactive) complex into a recombination active complex. In both cases, the species involved is unclear, and further work is required to determine the species involved. Furthermore, these results do not completely disprove the other models proposed for the boron oxygen degradation, although clearly those models will need to be adjusted to account for the ability to transition between the FRC and SRC shown in this work. To provide further evidence of a single defect being responsible for both fast and slow B-O related degradation, temperature dependent lifetime measurements and a range of doping densities should be used.

IV. SUMMARY

This paper gives new insights into the behaviour of the B-O defect. The impact of thermal annealing on fast and slow degradation was investigated. By modulating the dark annealing conditions on samples in which the defects were already fully formed, the fraction of fast and slow degradation during further carrier injection could be modulated. Dark annealing a pre-degraded wafer for a short duration at a sufficiently low temperature was shown to leave the silicon material in a state that could enable a rapid degradation of lifetime during subsequent illumination. For longer durations of annealing, the fraction of degradation that occurred in the fast time-scale was reduced. Increasing the dark annealing temperature also favoured a transition back to a state that caused subsequent degradation to occur in the slow time-scale. The activation energy for this transition was determined as $E_a = 0.91 \pm 0.10\,\text{eV}$ with a corresponding attempt frequency of $\nu \approx 2 \times 10^8/\text{s}$.

The modulation of the extent of degradation in the fast and slow time-scales had no measureable influence on the capture cross-section ratio or the total extent of degradation for the samples used in this study. Furthermore, the annihilation rate was not modulated regardless of whether the degradation occurred in the fast or slow time-scale. This strongly indicates the same recombination activity of what is generally attributed to the FRC and SRC in the literature. It is concluded here that the FRC and SRC are in fact the same defect. That is, only one defect is responsible for the fast and slow B-O related degradation, in agreement with our previous work.[42] A kinetic model was proposed based on our previous work,[42] whereby the reaction that is typically described as the formation of the SRC is a precursor reaction (formation of the Stage 2 defect precursor) to the reaction typically described as the formation of the FRC (defect formation). Here, two recombination inactive states exist in the silicon, with a third recombination active state. The multi-stage degradation occurs due to a mix of the two recombination-inactive states. Any population in the Stage 2 defect precursor state, A2, can rapidly form defects. The other recombination inactive state is the precursor of the Stage 2 defect precursor, namely, the Stage 1 defect precursor, state A1. Hence, any population in state A1 must undergo a slow transition into the state A2 before the more rapid defect formation reaction takes place.

Whilst the paper does not give any insight into whether the defect formation process occurs via a diffusion based or latent defect based mechanism, the new insights presented on the behaviour of the degradation question the current theories assuming two separate defects being responsible for boron-oxygen related degradation. This may assist with the identification of the species involved with B-O related degradation in the future.

ACKNOWLEDGMENTS

The authors would like to acknowledge Daniel Chen, Kyung Kim, Ly Mai, Hongzhao Li, and the MAiA processing team who assisted with wafer processing. This Program was supported by the Australian Government through the Australian Renewable Energy Agency (ARENA) and the Australian Center for Advanced Photovoltaics (ACAP). The views expressed herein are not necessarily the views of the Australian Government, and the Australian Government does not accept responsibility for any information or advice contained herein. The authors would like to thank the commercial partners of the ARENA 1-A060 project and the UK Institution of Engineering and Technology (IET) for their funding support for this work through the A.F. Harvey Engineering Prize.

[1]H. Fischer and W. Pschunder, "Investigation of photon and thermal induced change in silicon solar cells," in *Proceedings of the 10th IEEE Photovoltaic Specialists Conference* (1973), pp. 404–411.
[2]J. Knobloch, S. W. Glunz, V. Henninger, W. Warta, W. Wettling, F. Schomann, W. Schmidt, A. Endrös, and K. A. Münzer, "21% efficient solar cells processed from Czochralski grown silicon," in *Proceedings of the 13th European Photovoltaic Solar Energy Conference* (1995), pp. 9–12.
[3]H. Hashigami, M. Dhamrin, and T. Saitoh, "Characterization of the initial rapid decay on light-induced carrier lifetime and cell performance degradation of Czochralski-grown silicon," Jpn. J. Appl. Phys., Part 1 **42**(5A), 2564–2568 (2003).

[4]K. Bothe and J. Schmidt, "Electronically activated boron-oxygen-related recombination centers in crystalline silicon," J. Appl. Phys. **99**(1), 13701 (2006).
[5]K. Bothe, J. Schmidt, and R. Hezel, "Comprehensive analysis of the impact of boron and oxygen on the metastable defect in CZ silicon," in *Proceedings of 3rd World Conference on Photovoltaic Energy Conversion* (2003), Vol. 2, pp. 1077–1080.
[6]T. U. Nærland, H. Haug, H. Angelskår, R. Søndenå, E. S. Marstein, and L. Arnberg, "Studying light-induced degradation by lifetime decay analysis: Excellent fit to solution of simple second-order rate equation," IEEE J. Photovoltaics **3**(4), 1265–1270 (2013).
[7]T. Niewelt, J. Schön, W. Warta, S. W. Glunz, and M. C. Schubert, "Degradation of crystalline silicon due to boron—Oxygen defects," IEEE J. Photovoltaics **7**(1), 383–398 (2017).
[8]M. Forster, E. Fourmond, F. E. Rougieux, A. Cuevas, R. Gotoh, M. Forster, E. Fourmond, F. E. Rougieux, A. Cuevas, R. Gotoh, and K. Fujiwara, "Boron-oxygen defect in Czochralski-silicon co-doped with gallium and boron," Appl. Phys. Lett. **100**(4), 42110 (2012).
[9]J. Knobloch, S. W. Glunz, D. Biro, W. Warta, E. Schaffer, and W. Wettling, "Solar cells with efficiencies above 21% proccessed from Czochroalski grown silicon," in *Proceedings of the 25th IEEE Photovoltaic Specialists Conference, Washington, DC* (IEEE, 1996), pp. 405–408.
[10]J. Schmidt, A. G. Aberle, and R. Hezel, "Investigation of carrier lifetime instabilities in Cz-grown silicon," in *Proceedings of the 26th IEEE Photovoltaic Specialists Conference* (1997), pp. 13–18.
[11]B. Lim, K. Bothe, and J. Schmidt, "Deactivation of the boron–oxygen recombination center in silicon by illumination at elevated temperature," Phys. Status Solidi RRL **2**(3), 93–95 (2008).
[12]J. Schmidt, K. Bothe, and R. Hezel, "Formation and annihilation of the metastable defect in boron-doped Czochralski silicon," in *Proceedings of the 29th IEEE Photovoltaic Specialists Conference* (2002), pp. 178–181.
[13]B. Lim, F. Rougieux, D. Macdonald, K. Bothe, and J. Schmidt, "Generation and annihilation of boron–oxygen-related recombination centers in compensated p-and n-type silicon," J. Appl. Phys. **108**, 103722 (2010).
[14]J. Schmidt and K. Bothe, "Structure and transformation of the metastable boron- and oxygen-related defect center in crystalline silicon," Phys. Rev. B **69**(2), 24107 (2004).
[15]T. Schutz-Kuchly, J. Veirman, S. Dubois, and D. R. Heslinga, "Light-induced-degradation effects in boron–phosphorus compensated n-type Czochralski silicon," Appl. Phys. Lett. **96**(9), 93505 (2010).
[16]S. M. Kim, S. Chun, S. Bae, S. Park, M. G. Kang, H. Song, Y. Kang, H. Lee, and D. Kim, "Light-induced degradation and metastable-state recovery with reaction kinetics modeling in boron-doped Czochralski silicon solar cells," Appl. Phys. Lett. **105**(8), 83509 (2014).
[17]S. Rein, T. Rehrl, W. Warta, S. W. Glunz, and G. Willeke, "Electrical and thermal properties of the metastable defect in boron-doped czochralski silicon (Cz-Si)," in *Proceedings of the 17th European Photovoltaic Solar Energy Conference* (2001), p. 1555.
[18]K. Bothe and J. Schmidt, "Fast-forming boron-oxygen-related recombination center in crystalline silicon," Appl. Phys. Lett. **87**(26), 262108 (2005).
[19]K. Bothe, R. Hezel, and J. Schmidt, "Recombination-enhanced formation of the metastable boron—Oxygen complex in crystalline silicon complex in crystalline silicon," Appl. Phys. Lett. **83**(6), 1125–1127 (2003).
[20]D. W. Palmer, K. Bothe, and J. Schmidt, "Kinetics of the electronically stimulated formation of a boron-oxygen complex in crystalline silicon," Phys. Rev. B **76**(3), 35210 (2007).
[21]C. Möller and K. Lauer, "Light-induced degradation in indium-doped silicon," Phys. Status Solidi RRL **7**(7), 461–464 (2013).
[22]K. Bothe, J. Schmidt, and R. Hezel, "Effective reduction of the metastable defect concentration in boron-doped Czochralski silicon for solar cells," in *Proceedings of the 29th IEEE Photovoltaic Specialists Conference* (2002), pp. 194–197.
[23]H. Hashigami, Y. Itakura, T. Saitoh, H. Hashigami, Y. Itakura, and T. Saitoh, "Effect of illumination conditions on Czochralski-grown silicon solar cell degradation Effect of illumination conditions on Czochralski-grown silicon solar cell degradation," J. Appl. Phys. **93**(7), 4240–4245 (2003).
[24]A. Herguth, G. Schubert, M. Kaes, and G. Hahn, "A new approach to prevent the negative impact of the metastable defect in boron doped Cz silicon solar cells," in *Proceedings of the 4th IEEE World Conference on Photovoltaic Energy Conversion* (2006), pp. 940–943.
[25]S. Y. Lim, F. E. Rougieux, and D. Macdonald, "Boron-oxygen defect imaging in p-type Czochralski silicon," Appl. Phys. Lett. **103**(9), 92105 (2013).
[26]T. Mchedlidze and J. Weber, "Direct detection of carrier traps in Si solar cells after light-induced degradation," Phys. Status Solidi RRL **9**(2), 108–110 (2015).
[27]M. Forster, P. Wagner, J. Degoulange, R. Einhaus, G. Galbiati, F. Emile, A. Cuevas, and E. Fourmond, "Impact of compensation on the boron and oxygen-related degradation of upgraded metallurgical-grade silicon solar cells," Sol. Energy Mater. Sol. Cells **120**, 390–395 (2014).
[28]F. E. Rougieux, B. Lim, J. Schmidt, M. Forster, D. Macdonald, F. E. Rougieux, B. Lim, J. Schmidt, M. Forster, D. Macdonald, and A. Cuevas, "Influence of net doping, excess carrier density and annealing on the boron oxygen related defect density in compensated n-type silicon," J. Appl. Phys. **110**(6), 63708 (2011).
[29]A. Herguth, G. Schubert, M. Käs, and G. Hahn, "Investigations on the long time behavior of the metastable boron–oxygen complex in crystalline silicon," Prog. Photovoltaics Res. Appl. **16**(2), 135–140 (2008).
[30]T. U. Nærland, H. Angelskår, and E. S. Marstein, "Direct monitoring of minority carrier density during light induced degradation in Czochralski silicon by photoluminescence imaging," J. Appl. Phys. **113**(19), 0–7 (2013).
[31]L. I. Khirunenko, Y. V Pomozov, M. G. Sosnin, and A. V Duvanskii, "Boron-oxygen-related defect in silicon," Solid State Phenom. **178–179**, 178–182 (2011).
[32]J. Schmidt and A. Cuevas, "Electronic properties of light-induced recombination centers in boron-doped Czochralski silicon," J. Appl. Phys. **86**(6), 3175–3180 (1999).
[33]G. Krugel, W. Wolke, J. Geilker, S. Rein, and R. Preu, "Impact of hydrogen concentration on the regeneration of light induced degradation," Energy Procedia **8**, 47–51 (2011).
[34]J. H. Reiss, R. R. King, and K. W. Mitchell, "Characterization of diffusion length degradation in Czochralski silicon solar cells," Appl. Phys. Lett. **68**(23), 3302–3304 (1996).
[35]V. V. Voronkov and R. Falster, "Latent complexes of interstitial boron and oxygen dimers as a reason for degradation of silicon-based solar cells," J. Appl. Phys. **107**(5), 53509 (2010).
[36]T. Niewelt, J. Schön, J. Broisch, S. Mägdefessel, W. Warta, and M. C. Schubert, "A unified parameterization for the formation of boron oxygen defects and their electrical activity," Energy Procedia **92**, 170–179 (2016).
[37]V. V. Voronkov and R. Falster, "Permanent deactivation of boron-oxygen recombination centres in silicon," Phys. Status Solidi **253**(9), 1721–1728 (2016).
[38]V. V. Voronkov, R. Falster, K. Bothe, B. Lim, and J. Schmidt, "Lifetime-degrading boron-oxygen centres in p-type and n-type compensated silicon," J. Appl. Phys. **110**(6), 63515 (2011).
[39]J. D. Murphy, K. Bothe, V. V. Voronkov, and R. J. Falster, "On the mechanism of recombination at oxide precipitates in silicon," Appl. Phys. Lett. **102**(4), 42105 (2013).
[40]V. V. Voronkov, R. Falster, B. Lim, and J. Schmidt, "Boron-oxygen related lifetime degradation in p-type and n-type silicon.," J. Appl. Phys. **50**(5), 123–136 (2012).
[41]V. V. Voronkov, R. Falster, and A. V. Batunina, "Modelling lifetime degradation in boron-doped Czochralski silicon," Phys. Status Solidi Appl. Mater. Sci. **208**(3), 576–579 (2011).
[42]B. Hallam, M. Abbott, T. Nærland, and S. Wenham, "Fast and slow lifetime degradation in boron-doped Czochralski silicon described by a single defect," Phys. Status Solidi RRL **10**(7), 520–524 (2016).
[43]T. Niewelt, S. Mägdefessel, and M. C. Schubert, "Fast *in-situ* photoluminescence analysis for a recombination parameterization of the fast BO defect component in silicon," J. Appl. Phys. **120**(8), 85705 (2016).
[44]D. H. Macdonald, L. J. Geerligs, and A. Azzizi, "Iron detection in crystalline silicon by carrier lifetime measurements for arbitrary injection and doping," J. Appl. Phys. **95**(3), 1021–1028 (2004).
[45]V. V. Voronkov, R. J. Falster, J. Schmidt, K. Bothe, and A. Batunina, "Lifetime degradation in boron doped Czochralski silicon," ECS Trans. **33**(11), 103–112 (2010).
[46]A. Y. Liu and D. Macdonald, "Precipitation of iron in multicrystalline silicon during annealing," J. Appl. Phys. **115**(11), 114901 (2014).
[47]Z. Hameiri, N. Borojevic, L. Mai, N. Nandakumar, K. Kim, S. Winderbaum, and A. S. Preparation, "Should the refractive index at 633 nm be used to characterize silicon nitride films?," in *Proceedings of the 43rd IEEE Photovoltaic Specialists Conference* (2016), pp. 2900–2904.

[48]B. J. Hallam, S. R. Wenham, P. G. Hamer, M. D. Abbott, A. Sugianto, C. E. Chan, A. M. Wenham, M. G. Eadie, and G. Xu, "Hydrogen passivation of BO defects in Czochralski silicon," Energy Procedia **38**, 561–570 (2013).
[49]R. A. Sinton and A. Cuevas, "Contactless determination of current–voltage characteristics and minority-carrier lifetimes in semiconductors from quasi-steady-state photoconductance data," Appl. Phys. Lett. **69**(17), 2510–2512 (1996).
[50]H. Nagel, C. Berge, and A. G. Aberle, "Generalized analysis of quasi-steady-state and quasi-transient measurements of carrier lifetimes in semiconductors," J. Appl. Phys. **86**(11), 6218 (1999).
[51]S. W. Glunz, S. Rein, W. Warta, J. Knobloch, and W. Wettling, "Degradation of carrier lifetime in Cz silicon solar cells," Sol. Energy Mater. Sol. Cells **65**(1), 219–229 (2001).
[52]A. Richter, F. Werner, A. Cuevas, J. Schmidt, and S. W. Glunz, "Improved parameterization of Auger recombination in silicon," Energy Procedia **27**, 88–94 (2012).
[53]T. Niewelt, J. Schön, J. Broisch, W. Warta, and M. Schubert, "Electrical characterization of the slow boron oxygen defect component in Czochralski silicon," Phys. Status Solidi RRL **9**(12), 692–696 (2015).
[54]J. D. Murphy, K. Bothe, R. Krain, V. V. Voronkov, and R. J. Falster, "The impact of oxide precipitates on minority carrier lifetime in Czochralski silicon," ECS Trans. **50**(5), 137–144 (2013).
[55]S. Rein and S. W. Glunz, "Electronic properties of the metastable defect in boron-doped Czochralski silicon: Unambiguous determination by advanced lifetime spectroscopy," Appl. Phys. Lett. **82**(7), 1054–1056 (2003).
[56]B. Lim, V. V. Voronkov, R. Falster, K. Bothe, and J. Schmidt, "Lifetime recovery in p -type Czochralski silicon due to the reconfiguration of boron-oxygen complexes via a hole-emitting process," Appl. Phys. Lett. **98**(16), 162104 (2011).
[57]V. Voronkov and R. Falster, "The nature of boron-oxygen lifetime-degrading centres in silicon," Phys. Status Solidi **13**(10–12), 712–717 (2016).
[58]V. V. Voronkov and R. Falster, "Light-induced boron-oxygen recombination centres in silicon: Understanding their formation and elimination," Solid State Phenom. **206**, 3–14 (2014).
[59]P. Hamer, N. Nampalli, H. Ziv, M. Kim, D. Chen, N. Gorman, B. Hallam, M. Abbott, and S. Wenham, "Boron-oxygen defect formation rates and activity at elevated temperatures," Energy Procedia **92**, 791–800 (2016).